



# Reconstruction of the geomagnetic field between 20 and 60 kyr BP from cosmogenic radionuclides in the GRIP ice core

G. Wagner<sup>a,\*</sup>, J. Masarik<sup>b,1</sup>, J. Beer<sup>a,2</sup>, S. Baumgartner<sup>c,3</sup>, D. Imboden<sup>a,4</sup>,  
P.W. Kubik<sup>d,5</sup>, H.-A. Synal<sup>d,5</sup>, M. Suter<sup>e,5</sup>

<sup>a</sup> Swiss Federal Institute for Environmental Science and Technology (EAWAG), Überlandstrasse 133, CH-8600 Dübendorf, Switzerland

<sup>b</sup> Department of Nuclear Physics, Komensky University, Mlynska dolina F11 Sk-842 15 Bratislava, Slovakia

<sup>c</sup> Verein für Krebsforschung, Institut Hiscia, CH-4144 Arlesheim, Switzerland

<sup>d</sup> Paul Scherrer Institute, clo ETH Hönggerberg, CH-8093 Zürich, Switzerland

<sup>e</sup> Institute for Particle Physics, ETH Hönggerberg, CH-8093 Zürich, Switzerland

---

## Abstract

A pure physical model for the simulation of cosmic ray particle interactions with the Earth's atmosphere was used to investigate the effects of a changing geomagnetic field on the production rates of cosmogenic nuclides. Analytical dependencies of the production rates of <sup>3</sup>H, <sup>7</sup>Be, <sup>10</sup>Be, <sup>14</sup>C and <sup>36</sup>Cl on geomagnetic field intensity were developed. Applying those relations to the <sup>10</sup>Be and <sup>36</sup>Cl fluxes measured in the GRIP ice core, the geomagnetic field intensity for the period between 20 and 60 kyr BP was reconstructed. Comparison with remnant magnetism records from marine sediment cores shows excellent agreement. This validates the use of cosmogenic nuclides in ice cores to reconstruct geomagnetic field variations. © 2000 Elsevier Science B.V. All rights reserved.

**Keywords:** <sup>10</sup>Be and <sup>36</sup>Cl production rate; GRIP ice core; Paleogeomagnetic field

---

## 1. Introduction

The interaction of cosmic ray particles with the Earth's atmosphere leads to the production of a variety of cosmogenic nuclides. These cosmogenic nuclides have a wide range of applications in dating and tracing various events and processes in the environment. For most applications, it is very important to know the temporal variations of nuclide production rates in the past.

Several related factors can cause changes in the production rates of cosmogenic nuclides in the Earth's atmosphere. They include changes in the

---

\* Corresponding author. Tel.: +41-1-823-5316; fax: +41-1-823-5210.

*E-mail addresses:* gerhard.wagner@eawag.ch (G. Wagner), masarik@fmph.uniba.sk (J. Masarik), beer@eawag.ch (J. Beer), baumgartner@hisca.ch (S. Baumgartner), imboden@up.umhw.ethz.ch (D. Imboden), kubik@particle.phys.ethz.ch (P.W. Kubik), synal@particle.phys.ethz.ch (H.-A. Synal), suter@particle.phys.ethz.ch (M. Suter).

<sup>1</sup> Fax: +421-7-654-25-882.

<sup>2</sup> Fax: +41-1-823-5210.

<sup>3</sup> Fax: +41-61-706-7200.

<sup>4</sup> Fax: +41-1-632-1069.

<sup>5</sup> Fax: +41-1-633-1067.

galactic cosmic ray particle flux, changes in solar activity and variations in shielding by the Earth's magnetic field. It is often impossible to separate these different contributions in the observed variability of measured nuclide abundances. Very little is known about the variation of the galactic cosmic ray flux. Changes in solar modulation are also poorly known, except those related to the 11-yr Schwabe cycle. It is, therefore, difficult to establish the extent to which those two processes affect the production rate. However, there is evidence that on longer time scales, production rate variations are mainly caused by solar and geomagnetic modulation [1]. Nuclide concentrations in lunar samples indicate that the galactic cosmic ray flux, averaged over millions of years was constant within 20% [2].

As both galactic and solar cosmic rays consist mainly of charged particles, a large fraction of them is deflected by the Earth's magnetic field. Changes in the field intensity, therefore, control the fraction of the cosmic ray particles that enter the Earth's atmosphere and consequently the production rate of cosmogenic nuclides. Several studies employing Lal's relation between geomagnetic field intensity and production rate [3] were devoted to the investigation of geomagnetic field modulation of cosmogenic nuclide production rates in the atmosphere. Due to the lack of a precise knowledge of the geomagnetic field intensity in the past, the results obtained often agree only qualitatively [4,5]. A few recent papers dealt with this problem employing the McElhinny and Senanayake [6] data for the past 10 kyr and Tric et al. [7], Meynadier et al. [8], Guyodo and Valet [9] for older times. The investigated nuclides include  $^{14}\text{C}$  [10,11],  $^{36}\text{Cl}$  [12,13] and  $^{10}\text{Be}$  [14,15].

We report here on the investigations of the influence of geomagnetic field intensity changes on the production of cosmogenic nuclides in the Earth's atmosphere. They are based on a new relationship between production rate and field intensity obtained from a Monte Carlo simulation of the production processes involved.  $^{36}\text{Cl}$  and  $^{10}\text{Be}$  data from the GRIP ice core are interpreted in terms of geomagnetic field intensity variations using obtained model dependencies.

## 2. Model calculations

Our model for the simulation of the interaction of primary and secondary cosmic ray particles with matter is based on the GEANT [16] and MCNP [17] codes. As this code system is described in detail elsewhere [18], we repeat here only its main features, which are relevant for the present study. In our simulations, only primary protons with energies between 10 MeV and 100 GeV were considered. The characteristic feature of the particle interactions at these energies is the production of a cascade of secondary particles. For these calculations, the Earth's atmosphere was modeled as a spherical shell with an inner radius of 6378 km and a thickness of 100 km. The following elemental composition (in weight %) was used: 75% N, 23.2% O and 1.3% Ar. The atmospheric shell was divided into 34 subshells to account for the change in the atmospheric density. The total thickness of the atmosphere was  $1033 \text{ g cm}^{-2}$ .

The production rate of a cosmogenic nuclide  $j$  at depth  $D$  is

$$P_j(D) = \sum_i N_i \sum_k \int_0^\infty \sigma_{ijk}(E_k) J_k(E_k, D) dE_k, \quad (1)$$

where  $N_i$  is the number of atoms of a target element  $i$  per kg material in the sample,  $\sigma_{ijk}(E_k)$  the cross-section for the production of the cosmogenic nuclide  $j$  from the target element  $i$  by particles of type  $k$  with energy  $E_k$ , and  $J_k(E_k, D)$  is the flux of particles of type  $k$  with energy  $E_k$  at depth  $D$  inside the Earth's atmosphere. The particle fluxes  $J_k(E_k, D)$  were calculated with the GEANT/MCNP code system. The statistical errors of the calculations were on the level of 4–6%. The systematic uncertainties of our calculated fluxes are estimated to be in the range of 5–10% for depths less than  $400 \text{ g cm}^{-2}$  and increase with depth in the atmosphere. For the cross-sections  $\sigma_{ijk}$ , we relied on the values evaluated and tested in earlier calculations [19,20] and updated with new values from recent experiments [21–24]. In this paper, we present only the production rates originating from the interactions of galactic cosmic rays. Their flux varies in time. The dominant source of the variations is the solar and geomagnetic modulation. The solar

modulation is taken into account in the expression for the differential primary GCR proton flux [21]. Solar cosmic ray particles produce cosmogenic nuclides only at shallow depths in the atmosphere and at high latitude, where the geomagnetic field does not prevent them from entering the atmosphere [21]. The integral flux of protons with energies above 10 MeV used in these simulations is  $4.56 \text{ nucleons cm}^{-2} \text{ s}^{-1}$ . This value corresponds to the modulation parameter  $\phi = 550 \text{ MeV}$ , which is identical with the long-term average value determined from the cosmogenic nuclide data in lunar samples [19].

### 3. Geomagnetic modulation of the cosmogenic nuclide production

The magnetic field of the Earth deflects incoming cosmic ray particles depending on their magnetic rigidity  $R$  and the angle of incidence. The rigidity of a particle is defined as the momentum per unit charge  $R = pc/Ze$ , where  $p$  is the momentum,  $Ze$  the charge of the particle and  $c$  is the

velocity of light. For each angle of incidence, there is a critical rigidity below which the incoming particle cannot reach the Earth's atmosphere.

We used the world grid of calculated cosmic ray vertical cut-off rigidities for the year 1980 [25] to determine the non-vertical cut-offs. Paleomagnetic data show that the geomagnetic field intensity has varied from almost zero to about two times of its current value [9,26] during the last 200 kyr. To cover this whole range of geomagnetic field intensities in our calculations, we varied its value from zero to two times of its present value in steps of 0.25. The shape of the field was fixed in all our simulations.

The latitudinal dependence of the depth integrated  $^{10}\text{Be}$  production rate on the geomagnetic field intensity for an average solar modulation  $\phi = 550 \text{ MeV}$  is presented in Fig. 1. Similar production rate patterns hold for all investigated nuclides and for all values of the solar modulation parameter  $\phi$ . The difference between the highest depth integrated production rate (latitude range  $60\text{--}90^\circ$ ) and the lowest production rate (latitude range  $0\text{--}10^\circ$  and field intensity two times of its

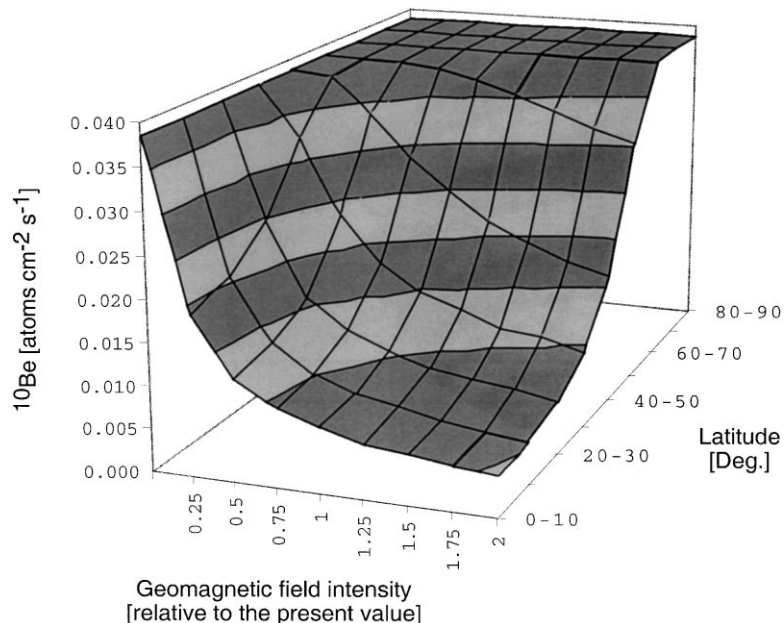


Fig. 1. Dependence of  $^{10}\text{Be}$  production rate on latitude and geomagnetic field intensity for the long-term average solar modulation parameter  $\phi = 550 \text{ MeV}$ .

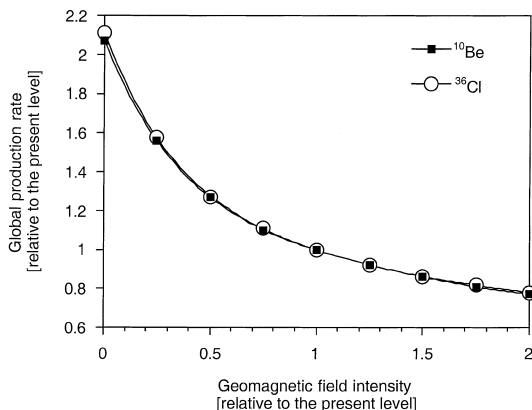


Fig. 2. Dependence of relative  $^{10}\text{Be}$  and  $^{36}\text{Cl}$  global average production rate on geomagnetic field intensity for the long-term average solar modulation parameter  $\phi = 550$  MeV.

current value) is about a factor of 8 for spallogenic nuclides and a factor of 9 for  $^{14}\text{C}$ .

The global average production rates for the present field intensity and modulation parameter  $\phi = 550$  MeV are 0.281, 0.0354, 0.0184, 2.02 and 0.00188 atoms  $\text{cm}^{-2} \text{s}^{-1}$  for  $^3\text{H}$ ,  $^7\text{Be}$ ,  $^{10}\text{Be}$ ,  $^{14}\text{C}$  and  $^{36}\text{Cl}$ , respectively. Fig. 2 shows the calculated production rates of  $^{10}\text{Be}$  and  $^{36}\text{Cl}$  as a function of the geomagnetic field intensity  $B$  for the solar modulation parameter  $\phi = 550$  MeV. The dependence  $j$  of production rates of all investigated nuclides on geomagnetic field intensity  $B$  can be fitted by a polynomial of fifth degree  $P_j(B) = a_j + b_j * B + c_j * B^2 + d_j * B^3 + e_j * B^4 + f_j * B^5$ . The coefficients  $a$ ,  $b$ ,  $c$ ,  $d$ ,  $e$  and  $f$  are summarized in Table 1 for  $^{10}\text{Be}$ ,  $^{14}\text{C}$  and  $^{36}\text{Cl}$ . The absolute values of the coefficients depend on the nuclide, but the ratios of the production rates of spallogenic nuclides such as  $^7\text{Be}$ ,  $^{10}\text{Be}$  and  $^{36}\text{Cl}$  are, within the statistical errors of the calculations, independent of solar modulation and geomagnetic

field intensity. The ratios are 9.8 for  $^{10}\text{Be}/^{36}\text{Cl}$  and 1.9 for  $^7\text{Be}/^{10}\text{Be}$ .

#### 4. Geomagnetic modulation of the $^{10}\text{Be}$ and $^{36}\text{Cl}$ flux in the summit GRIP ice core and derivation of the geomagnetic field from the $^{10}\text{Be}$ and $^{36}\text{Cl}$ flux

As the agreement of calculated and measured nucleon fluxes in the Earth's atmosphere is reasonable (for compared latitudes and altitudes, fluxes differ not more than 7%) [18], we used our model to investigate the relationship between the variability of the  $^{10}\text{Be}$  and  $^{36}\text{Cl}$  data from the Summit GRIP ice core and past changes in the geomagnetic field. 1350  $^{10}\text{Be}$  and 1080  $^{36}\text{Cl}$  measurements were performed on ice samples providing excellent data sets with a high temporal resolution for the last 100 kyr [27,28]. The  $^{10}\text{Be}$  measurements were carried out in a joint project between Raisbeck and Yiou (Paris) and our group, whereas the  $^{36}\text{Cl}$  measurements were all made by our group in Zürich.

The decay corrected  $^{10}\text{Be}$  and  $^{36}\text{Cl}$  concentrations in an ice core are the result of the interplay between three processes: production, transport and deposition. As our model predicts only the production rate of  $^{10}\text{Be}$  and  $^{36}\text{Cl}$ , we tried to eliminate the influence of the two other processes by converting radionuclide concentrations into fluxes [12]. At least for the marine isotope stages 3 (MIS-3), our method seems to work. The low correlation between the  $^{10}\text{Be}$  and  $^{36}\text{Cl}$  fluxes and the snow accumulation rate ( $r^2 \leq 4\%$  for MIS-3) indicates that a possible deposition effect was successfully eliminated (Table 2) [29,30]. Similarly, a transport effect caused by changes in the air mass changes should also be eliminated, because the fluxes of  $^{10}\text{Be}$  and  $^{36}\text{Cl}$  are almost independent of

Table 1

Coefficients of fifth degree polynomial describing the dependence of cosmogenic nuclide production rate on geomagnetic field intensity<sup>a</sup>

Nuclide	$a$	$b$	$c$	$d$	$e$	$f$
$^{10}\text{Be}$	2.07	-2.649	2.838	-1.741	0.549	-0.069
$^{14}\text{C}$	2.381	-2.644	1.852	-0.738	0.17	-0.02
$^{36}\text{Cl}$	2.111	-2.813	3.166	-2.089	0.725	-0.102

<sup>a</sup> The  $^{10}\text{Be}$ ,  $^{14}\text{C}$  and  $^{36}\text{Cl}$  production rates are normalized to the present field intensity and the solar modulation parameter 550 MeV.

Table 2

Shared variance (correlation coefficients  $r$  in square) between the  $^{10}\text{Be}$ -flux, the  $^{36}\text{Cl}$ -flux, on the one hand, and the accumulation rate on the other hand, during the different MIS stages of the last 100 kyr BP

	$r^2$ (Acc., $^{10}\text{Be}$ flux) (%)	$r^2$ (Acc., $^{36}\text{Cl}$ flux) (%)
MIS-1	2.2	1
MIS-2	14	8.4
MIS-3	1.4	4
MIS-4	2.9	29
MIS-5(a–c)	40	9

the mid- to low-latitude circulation index (MLCI) and the polar circulation index (PCI) ( $r^2 \leq 1\%$  for MIS-3) Table 3, Fig. 3 [31]. The decay corrected  $^{10}\text{Be}/^{36}\text{Cl}$ -ratios shown in Fig. 3 and Table 3, being only a function of atmospheric transport and therefore an index for transport changes of the radionuclides  $^{10}\text{Be}$  and  $^{36}\text{Cl}$ , are also almost independent of the MLCI and PCI during MIS-3 (Table 3, Fig. 3). Tables 2 and 3 show that only during the MIS-3, the fluxes of  $^{10}\text{Be}$  and  $^{36}\text{Cl}$  seem to be independent ( $r^2 \leq 4\%$ ) of atmospheric transport and deposition. Therefore, only in this time period, the  $^{10}\text{Be}$  and  $^{36}\text{Cl}$  fluxes are controlled predominantly by the production. In consequence, we restrict the reconstruction of the geomagnetic field to this time interval (MIS-3). Earlier, NRM and  $^{10}\text{Be}$  derived geomagnetic paleointensity data, deduced from ocean sediments over the last 200 kyr, are perhaps not free of climatic influences [32].

To reconstruct the geomagnetic field from the  $^{10}\text{Be}$  and  $^{36}\text{Cl}$  fluxes, we assume that the  $^{10}\text{Be}$  and  $^{36}\text{Cl}$  fluxes at the Summit during the MIS-3 are linearly related to their average global production rate. Justification for this assumption is based on the characteristics of its geographical location, since Central Greenland receives a substantial part of its precipitation from lower latitudes [33] and many chemical species found in the ice originate from source regions in North America or Europe [31].

The combined  $^{10}\text{Be}$  and  $^{36}\text{Cl}$  flux for the last ice age (17.5–100 kyr BP) is shown in Fig. 3(a). Also shown are the individual  $^{10}\text{Be}$  and  $^{36}\text{Cl}$  fluxes in Fig. 3(b). The graphs in Fig. 3(c) and (d) show the  $^{10}\text{Be}/^{36}\text{Cl}$  ratios and MLCI. The combined  $^{10}\text{Be}$  and  $^{36}\text{Cl}$  flux data presented in Fig. 3(a) were obtained applying the following procedures.  $^{10}\text{Be}$  and  $^{36}\text{Cl}$  flux data were independently, linearly interpolated using a time step of 100 yr, low pass filtered (cut-off frequency =  $1/3000 \text{ yr}^{-1}$ ), and normalized to their mean value during the time interval between 17.5 and 100 kyr BP. The normalized  $^{10}\text{Be}$  and  $^{36}\text{Cl}$  fluxes were arithmetically averaged. The averaging of  $^{10}\text{Be}$  and  $^{36}\text{Cl}$  was applied to eliminate small transport effects influencing the measured concentrations of particular nuclides. This approach is justified by results of model simulations (see previous part), which showed the  $^{10}\text{Be}/^{36}\text{Cl}$  ratio to be independent of geomagnetic field intensity. A comparison between the measured and the calculated  $^{10}\text{Be}/^{36}\text{Cl}$  ratio reveals a factor 2.5. There are several hypotheses, but no final answer yet for this discrepancy. However, for our purpose, the crucial point is that

Table 3

Shared variance (correlation coefficients  $r$  in square) between the  $^{10}\text{Be}$  flux, the  $^{36}\text{Cl}$  flux, the  $^{10}\text{Be}/^{36}\text{Cl}$  (decay corrected) on the one hand, and the MLCI and PCI on the other hand, during the different MIS stages of the last 100 kyr BP<sup>a</sup>

	$r^2$ (MLCI, $^{10}\text{Be}/^{36}\text{Cl}$ ) (%)	$r^2$ (MLCI, $^{10}\text{Be}$ ) (%)	$r^2$ (MLCI, $^{36}\text{Cl}$ ) (%)	$r^2$ (PCI, $^{10}\text{Be}/^{36}\text{Cl}$ ) (%)	$r^2$ (PCI, $^{10}\text{Be}$ ) (%)	$r^2$ (PCI, $^{36}\text{Cl}$ ) (%)
MIS-1	34	4	23	1.7	2.3	3.6
MIS-2	0.36	0.01	2	2	0.5	0.04
MIS-3	0.04	0.09	0.09	0.36	0.04	1
MIS-4	2	10	5.3	18.5	4	0.5
MIS-5(a–c)	7.3	23	4	4	6.3	1

<sup>a</sup> Only during MIS-3 the shared variances are less than or equal to 1%.

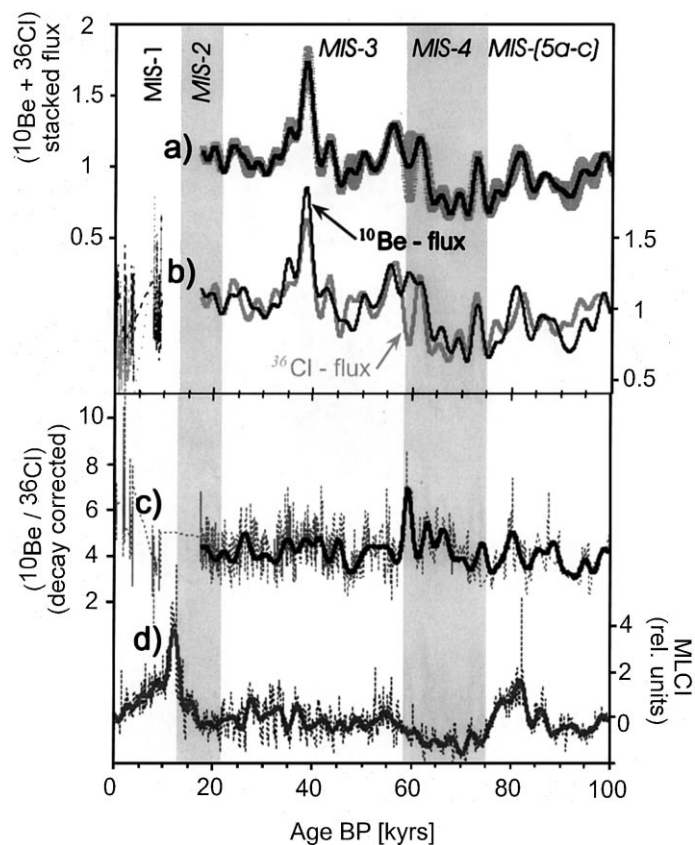


Fig. 3. (a) Averaged  $^{10}\text{Be}$  plus  $^{36}\text{Cl}$  flux calculated from the measured  $^{10}\text{Be}$  and  $^{36}\text{Cl}$  concentrations in GRIP ice core as a function of time. (b)  $^{10}\text{Be}$  plus  $^{36}\text{Cl}$  flux as a function of time [29]. (c) Decay-corrected  $^{10}\text{Be}/^{36}\text{Cl}$  ratio as a function of time. (d) MLCI as a function of time.

we are only making use of the flux changes, which are very similar for  $^{10}\text{Be}$  and  $^{36}\text{Cl}$  (Fig. 3(b)). A constant offset is removed when normalizing the data. The uncertainty of the resulting averaged  $^{10}\text{Be}$  plus  $^{36}\text{Cl}$  flux is the S.D. of the arithmetic mean value. In cases when this S.D. is smaller than the error calculated by error propagation, we choose the latter error. The error of the interpolated  $^{10}\text{Be}$  flux is estimated to be 7% and the one of the interpolated  $^{36}\text{Cl}$  flux 8%, respectively. These are the mean errors of the accelerator mass spectrometry (AMS) analyses.

Fig. 4 shows the geomagnetic field intensity during MIS-3, reconstructed from the combined  $^{10}\text{Be}$  and  $^{36}\text{Cl}$  flux in the GRIP ice core. The shaded area indicates the uncertainty in the cal-

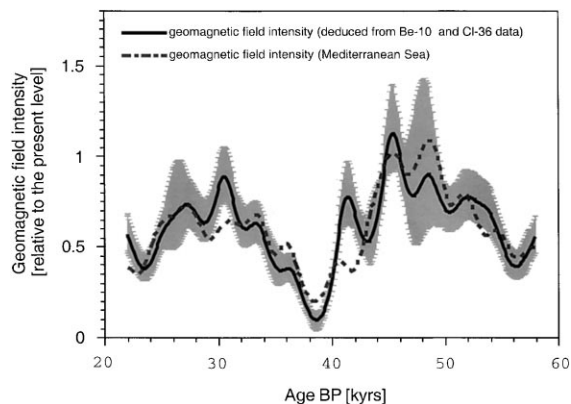


Fig. 4. Geomagnetic field intensity as reconstructed from the Mediterranean sea sediments [7] and as calculated from our averaged  $^{10}\text{Be}$  plus  $^{36}\text{Cl}$  flux data.

culated field intensity. Also shown is the field measured on a Mediterranean sediment core [7]. The correlation between the geomagnetic field intensities obtained from these two independent reconstructions is very high ( $r^2 = 70\%$ ). For comparison, we chose the reconstructed magnetic field from the Mediterranean sediment [7], because of its high time resolution and its good agreement with the stacked magnetic field curve, reconstructed by 18 different ocean sediment cores [9]. Since the two records are based on independent but uncalibrated time scales, we adjusted arbitrarily the sediment time scale to match the one of the GRIP ice core [29] (Fig. 5). The maximum age shift is about 11%. This is still within the uncertainties of the original time scales. In our calculation of the geomagnetic field intensity, the combined  $^{10}\text{Be}$  and  $^{36}\text{Cl}$  flux was normalized in such a way, that for the minimum of the calculated geomagnetic field intensity at about 40 kyr BP (Laschamp event) a value of 10% of its current value is assumed. The normalization is supported also by new data from the Atlantic ocean [34].

In comparison with other methods, the reconstruction of the geomagnetic field intensity based on  $^{10}\text{Be}$  and  $^{36}\text{Cl}$  concentrations in ice cores has two advantages. Firstly, it is sensitive mainly to the dominant dipole moment, because the shielding effect of the non-dipolar moments decreases faster

with increasing distance from the Earth. Secondly, the radioisotope technique is especially sensitive to variations of weak fields, because the weaker the field, the stronger the production effect for a field change (Fig. 2).

## 5. Conclusions

In the recent past, the number of applications of cosmogenic nuclides has steadily increased [11]. However, to make full use of their potential, a quantitative understanding of their production processes is necessary. With a new model using the particle production and transport simulation codes GEANT and MCNP, it is now possible to calculate not only the mean global production rates but also their spatial and temporal variations. Based on this model, the dependence of the production rate of cosmogenic nuclides in the Earth's atmosphere on solar modulation and geomagnetic field intensity was derived.

The  $^{10}\text{Be}$  and the  $^{36}\text{Cl}$  records from the GRIP ice core have been interpreted in terms of changes of the geomagnetic dipole moment. Strong changes of the paleogeomagnetic field intensity, found by paleomagnetic studies such as the Laschamps event [7–9] are reflected by a substantial increase of the  $^{10}\text{Be}$  and  $^{36}\text{Cl}$  production rate. Taking the measured, low pass filtered  $^{10}\text{Be}$  and  $^{36}\text{Cl}$  concentrations in the Summit GRIP ice core, calculating the combined  $^{10}\text{Be}$  and  $^{36}\text{Cl}$  flux, assuming that the geomagnetic field intensity of the Laschamp event was 10% of its current value, and using our model calculations, the intensity of the geomagnetic field in the past is determined. To minimize climatic and atmospheric transport effects, the investigations were restricted to time periods, in which the  $^{10}\text{Be}$  and the  $^{36}\text{Cl}$  flux are most probably independent of the air mass circulation and of the accumulation rate. These results, together with a similar reconstruction based on  $^{10}\text{Be}$  in globally stacked deep sea sediments [15] validate the cosmogenic nuclides as a new independent tool for the reconstruction of the geomagnetic field intensity in the past.

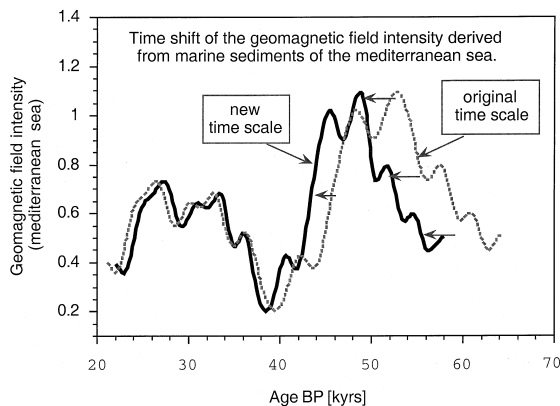


Fig. 5. Illustration of time scale shifting employed to match the two records presented in Fig. 4.

## Acknowledgements

This work is a contribution to the Greenland Ice Core Project (GRIP) organized by the European Science Foundation. We wish to thank C. Stengel, E. Meili, S. Bollhalder and A. Lück for their valuable laboratory work and for the data reduction. We also acknowledge the major support by the staff of the PSI/ETH AMS facility. We thank P. Mayewski for providing the MLCI and PCI data. This work was supported by the Swiss National Science Foundation.

## References

- [1] M. Stuiver, T.F. Braziunas, B. Becker, B. Kromer, *Quat. Res.* 35 (1991) 1.
- [2] S. Vogt, G.F. Herzog, R.C. Reedy, *Rev. Geophys.* 28 (1990) 253.
- [3] D. Lal, in: G.C. Castagnoli (Ed.), North-Holland, Amsterdam, 1988 pp. 215–233.
- [4] M. Barbetti, K. Flude, *Nature* 279 (1979) 202.
- [5] E. Bard, B. Hamelin, R.G. Fairbanks, A. Zindler, *Nature* 345 (1990) 405.
- [6] M.W. McElhinny, W.E. Senanayake, *J. Geomag. Geoelect.* 34 (1982) 39.
- [7] E. Tric, J.P. Valet, P. Tucholka, M. Paterne, L. LaBeyrie, F. Guichard, L. Tauxe, M. Fontugne, *J. Geophys. Res.* 97 (1992) 9337.
- [8] L. Meynadier, J.P. Valet, R. Weeks, N.J. Shackleton, V. Lee Hagee, *Earth Planet. Sci. Lett.* 114 (1992) 39.
- [9] Y. Guyodo, J.P. Valet, *Earth Planet. Sci. Lett.* 143 (1996) 23.
- [10] A. Mazaud, C. Laj, E. Bard, M. Arnold, E. Tric, *Geophys. Res. Lett.* 18 (1991) 1885.
- [11] E. Bard, *Science* 277 (1997) 532.
- [12] S. Baumgartner, J. Beer, J. Masarik, G. Wagner, L. Meynadier, H.-A. Synal, *Science* 279 (1998) 1330.
- [13] M.A. Plummer, F.M. Phillips, J. Fabryka-Martin, H.J. Turin, P.E. Wigand, P. Sharma, *Science* 277 (1997) 538.
- [14] A. Mazaud, C. Laj, M. Bender, *Geophys. Res. Lett.* 21 (1994) 337.
- [15] M. Frank, B. Schwarz, S. Baumann, P.W. Kubik, M. Suter, A. Mangini, *Earth Planet. Sci. Lett.* 149 (1997) 121.
- [16] B. Brun, GEANT3 User's guide, Report DD/EE/84-1 584, 1987.
- [17] J.F. Briesmeister, MCNP – A general Monte Carlo N-particle transport code version 4A, LA-12625-M, LANL, Los Alamos 693, 1993.
- [18] J. Masarik, J. Beer, *J. Geophys. Res.* 104 (1999) 12099.
- [19] J. Masarik, R.C. Reedy, *Geochim. Cosmochim. Acta* 58 (1994) 5307.
- [20] J. Masarik, R.C. Reedy, *Earth Planet. Sci. Lett.* 136 (1995) 381.
- [21] R. Bodemann et al., *Nucl. Instr. and Meth. B* 82 (1993) 9.
- [22] D. Huggle et al., *Planet. Space Sci.* 44 (1996) 147.
- [23] R. Michel et al., *Nucl. Instr. and Meth. B* 103 (1995a) 182.
- [24] R. Michel et al., *Nucl. Instr. and Meth. B* 129 (1997) 153.
- [25] M.A. Shea, D.F. Smart, in: *Proceedings of the 18th ICRC* 3, 1983, p. 514.
- [26] A. Bucha, *Nature* 224 (1969) 681.
- [27] F. Yiou et al., *J. Geophys. Res.* 102 (1997) 26783.
- [28] S. Baumgartner, J. Beer, M. Suter, B. Dittrich-Hannen, H.-A. Synal, P.W. Kubik, C. Hammer, S. Johnsen, *J. Geophys. Res.* 102 (1997) 26659.
- [29] S.J. Johnsen, D. Dahl-Jensen, W. Dansgaard, N. Gundestrup, *Tellus B* 47 (1995) 624.
- [30] R.B. Alley, R.C. Finkel, K. Nishiizumi, S. Anandakrishnan, C.A. Shuman, G. Mershon, G.A. Zielinski, P.A. Mayewski, *J. Glacio.* 41 (1995) 503.
- [31] P.A. Mayewski, L.D. Meeker, M.S. Twickler, S. Whitlow, Q. Yang, W.B. Lyons, M. Prentice, *J. Geophys. Res.* 102 (1997) 26345.
- [32] Y.S. Kok, *Earth Planet. Sci. Lett.* 166 (1999) 105.
- [33] S.J. Johnsen, W. Dansgaard, J.W.C. White, *Tellus B* 41 (1989) 452.
- [34] C. Laj, C. Kissel, A. Maraud, J.E.T. Channel, J. Beer, *Phil. Trans. R. Soc. Lond. A* 358 (2000) 1009.